PCCP

PAPER

View Article Online
View Journal | View Issue

Cite this: *Phys. Chem. Chem. Phys.*, 2019, **21**, 19469

Dynamics of TMAO and urea in the hydration shell of the protein SNase

Vladimir Voloshin,[a] Nikolai Smolin,[b] Alfons Geiger,[c] Roland Winter *[c] and Nikolai N. Medvedev *[ad]

Using all-atom molecular dynamics simulations of aqueous solutions of the globular protein SNase, the dynamic behavior of water molecules and cosolvents (trimethylamine-*N*-oxide (TMAO) and urea) in the hydration shell of the protein was studied for different solvent compositions. TMAO is a potent protein-stabilizing osmolyte, whereas urea is known to destabilize proteins. For molecules that are initially located in successive narrow layers at a given distance from the protein, the mean displacements and the distribution of displacements for short time intervals are calculated. For molecules that are initially located in solvation shells of a given thickness around the protein, the characteristic residence times in these shells are determined to characterize the dynamic behavior of the solvent molecules as a function of the distance to the protein. A combined consideration of these characteristics allows to reveal additional features of the dynamics of the cosolvents. It is shown that TMAO molecules leave the nearest vicinity of the protein faster than urea molecules, despite the fact that the mobility of TMAO molecules, measured by their mean displacements, is lower than that of urea. Moreover, we show that the rate of release of TMAO molecules from the hydration shell is lower in ternary (TMAO + urea + H_2O) solvent mixtures than in the binary ones. This is consistent with a recent observation that the fraction of TMAO near the protein decreases in the presence of urea. From the analysis of the decay of the number of particles initially located in the region of the first peak of the distribution function of solvent molecules around the protein, we estimated that about 20 water molecules and 6–7 urea molecules stay near the protein for more than 1000 ps.

Received 5th June 2019,
Accepted 20th August 2019

DOI: 10.1039/c9cp03184g

rsc.li/pccp

1. Introduction

Recently, we studied in detail the distribution of the cosolvent molecules trimethylamine-*N*-oxide (TMAO) and urea near the globular protein SNase in aqueous solution.[1] Large all-atom molecular dynamics (MD) models with different compositions of the solvent were studied. It was shown that the fraction of the volume occupied by urea near the protein is significantly higher than its average in the bulk of the solution. At the same time, the fraction of the volume occupied by TMAO near the protein is approximately the same as in the bulk. It was also shown that the distribution of urea molecules near the protein remains unchanged upon addition of TMAO, while the fraction of TMAO near the protein decreases upon the addition of urea. The interest in these molecules is due to the fact that their presence affects the conformational equilibrium of proteins. Generally, the stability of proteins in aqueous solution and also their reactions and interactions are influenced by the addition of cosolvents, such as compatible osmolytes, which are also prevailing in biological cells. Methylamines, polyols, carbohydrates or amino acids are able to stabilize the native state of proteins and are therefore often designated as chemical chaperones. An important example is trimethylamine-*N*-oxide (TMAO), which is able to effectively stabilize the native state of proteins and compensates deteriorating effects of temperature, pressure, and urea.[2–4] Other cosolvents, denaturants like urea, interact preferentially with the protein, thereby destabilizing proteins and hence favor the unfolded state of proteins.[3,4] Computer modelling is widely used to study the molecular mechanisms underlying the effects of these cosolutes on proteins.[3,5–7] It is believed that urea interacts directly with the protein, causing a weakening of the intramolecular bonds that keep the protein in a folded state.[7] The mechanism of TMAO is more complex: it is assumed that TMAO affects the protein indirectly through water.[8] As TMAO strongly interacts with the surrounding water, it has a less effect on intramolecular bonds

[a] *Institute of Chemical Kinetics and Combustion, SB RAS, 630090 Novosibirsk, Russia. E-mail: nikmed@kinetics.nsc.ru*
[b] *Department of Cell and Molecular Physiology, Loyola University Chicago, Maywood, Illinois 60153, USA*
[c] *Physikalische Chemie, Fakultät für Chemie und Chemische Biologie, Technische Universität Dortmund, Otto-Hahn-Straße 4a, 44221 Dortmund, Germany. E-mail: roland.winter@tu-dortmund.de*
[d] *Novosibirsk State University, 630090 Novosibirsk, Russia*

of the protein and its specific hydration shell prevents it from residing close to the protein interface.[9,10] The reduced probability of finding TMAO in the vicinity of a protein is interpreted as an "osmophobic effect",[11] which, from a thermodynamic point of view, is considered to be the universal reason that osmolyte-protectors prevent the denaturation of proteins by temperature or pressure. The mechanism of counteraction to the denaturing effect of urea remains unclear, however. It has been assumed that there are strong hydrogen bonds between TMAO and urea, due to which the effect of urea on the protein weakens in the presence of TMAO.[12] It was also noted that TMAO counteracts urea by displacing it from the surface of amino acids.[13] On the other hand, it was shown by Smolin *et al.*[1] that the addition of TMAO to the solution does not affect the distribution of urea near the protein significantly. The mutual interaction of these osmolyte molecules in an aqueous solution in the absence of protein was studied by Kadtzyn *et al.*[14] The analysis of their molecular dynamics models of binary and ternary solutions of these osmolytes showed that the radial distribution functions for each component are not sensitive to the presence of the other component. Altogether, so far no clear-cut picture has emerged for the mutual influence of TMAO and urea in the presence of proteins.

Additional clarity in solving this problem may be expected by studying the dynamic behavior of the cosolvent molecules close to the protein, since in the aforementioned papers only structural properties have been explored. Dynamic properties of the hydration shells of proteins, DNA and lipid membranes have been studied by both experimental and theoretical methods (see for example the reviews ref. 15 and 16). However, the focus of these works was mainly on the study of water itself or on its interaction with proteins. It has been shown that the translational, rotational, and vibrational properties of water molecules near a protein differ from their properties in bulk solution. This is explained both by steric effects imposed by the complex and corrugated surface structure of protein molecules and by the direct interaction of water with the protein, which is also of complex nature. In addition to electrostatic and dispersive interactions, hydrogen bonds and hydrophobic interactions with non-polar groups play a significant role, which leads to a slowing down of water dynamical properties near the protein interface compared with water in the bulk. It has also been noted that such changes occur in a rather narrow spatial region of only a few molecular layers of water molecules around the protein.[16]

We emphasize that the calculation of dynamic characteristics of molecules, such as self-diffusion coefficients, velocity auto-correlation functions, and relaxation times, requires the analysis of a sufficiently long time interval of the molecular dynamics trajectories. However, during this time, some (or all) molecules that were originally in the hydration shell, may leave it. This essentially distinguishes the determination of the dynamic properties of water in hydration shells from the study of the molecular dynamics in homogeneous liquids and glasses. This problem has already been faced in the first MD simulation studies of the hydration properties of simple solutes[17,18] and a protein.[19] The mean square displacement of hydration water molecules has been calculated by several groups; see for example.[20–24] A nonlinear behavior of the Einstein plot is observed here, which is associated with the peculiarities of the dynamics of water near the macromolecule. The exit of the water molecules from the region of the hydration shell during the calculation is usually not discussed. The authors of ref. 24 suggest that the majority of waters remains within the hydration layer up to a few tens of ps, based on the conclusion that the observed Einstein plots are consistently linear in a certain period of time (t = 20 to 60 ps). This conclusion is debatable, however. A nonlinear behavior of the Einstein plot in the intermediate time interval can be related to an inhomogeneity of the system.[25–28] As discussed in ref. 28, for the diffusion coefficient of liquids confined to cavities or in inhomogeneous regions, neither the Einstein relation nor the Kubo relation are valid approaches. In such systems, molecules will stay in a given region only for a finite time and will then explore other regions. Since the dynamics of the molecule is different for different regions, the time dependence of the mean square displacement will become linear only at times long enough for the molecules to sample all regions, and then its slope will yield the diffusion coefficient averaged over the entire system. For the simplest situation of a plane interface of a liquid with a gas or solid, a general methodology was proposed for calculating the self-diffusion tensor from MD simulation using anisotropic Smoluchowski equations.[28] Hence, the dynamic properties of the hydration shell of proteins are obviously much more complex than envisaged before, as emphasized in a recent review on the water dynamics in the hydration shell of biomolecules,[16] which points also out that the dynamic characteristics calculated for molecules in the hydration shell have to be interpreted with great care.

It is a well-known fact that cosolvents can also have a marked effect on the conformational dynamics, ligand binding, the activity and intermolecular interactions of proteins.[4,7,29–36] For example, the influence of small cosolvent molecules on the occupancy of conserved water in bromodomains was studied by Caflisch *et al.*,[33] and general cosolvent effects on the aqueous solubility of nonpolar solutes, hydrophobic interactions, and the hydrophobic self-assembly/collapse of polymers are discussed in ref. 34 and 35. Herein, in continuation of our previous works,[37,38] we study the dynamics of both, water and cosolvent molecules (urea and TMAO) near the globular protein SNase as a function of distance from its surface. A novel contribution of this work is the simultaneous study of both water and cosolvent in the hydration layer, particularly given the contrast in the effects of the two different types of co-solvents that were evaluated. First, to estimate the mobility, we employ the self-part of the van Hove correlation function,[39,40] applying it to molecules starting in narrow layers at given distances from the protein, however. We then calculate the mean displacement during a fixed period of time for molecules that are initially located at a given distance from the protein. This allows one to judge the mobility of molecules depending on the distance to the protein. To estimate the residence time ("lifetime") of molecules near the protein, we monitor the average number of molecules which leave (respectively stay in) shells of different thicknesses around

the protein. A joint consideration of these different dynamic characteristics helps us to reveal the dynamic behavior of all solvent molecules near the protein.

2. Models

For the present analysis, we used all-atom molecular dynamics simulation models which have been obtained earlier in ref. 1. These systems contain one SNase protein molecule in a box with periodic boundary conditions, surrounded by water with the cosolvents urea and TMAO at different concentrations. Equilibrium simulations were carried out for an *NPT* ensemble, using the GROMACS software package.[41,42] Here, we analysed simulation runs at a temperature of 300 K and a pressure of 1 bar. The OPLS force field for the protein[43] and the SPC/E water model[44] were used. The force fields for urea and for TMAO were taken from ref. 8 and 45. For more information on the force fields and the simulation details see ref. 1. Here, solutions of the following compositions were used: (1) pure water (without cosolvents), (2) binary solutions of urea at concentrations of 1 M and 2 M, (3) binary solutions of TMAO at concentrations of 0.5 M and 1 M, and (4) ternary solutions with 0.5 M TMAO + 1 M urea and 1 M TMAO + 2 M urea. Every 2 ps, configurations of the final 40 ns of the full trajectories were used for the analysis (the total production run was 100 ns (ref. 1)), which provides reliable averaging of the characteristics studied.

Please note that our models are rather large. The average size of the box is 9.2 nm. In all cases, the protein molecule occupies less than 3% of the volume of the box. In the absence of cosolvents, 26 170 water molecules surround the protein. To generate models with cosolvents, some water molecules were replaced by the corresponding number of cosolvent molecules: 500 and 1000 urea molecules to obtain the 1 M and 2 M urea concentration; 250 and 500 TMAO molecules for the 0.5 M and 1 M TMAO concentration. For the ternary solvent compositions, the corresponding amounts of TMAO and urea molecules were added at the same time (*e.g.*, 500 TMAO, 1000 urea, and 20 106 water molecules). The initial size of the box was identical at the start of all simulations. During the equilibration period, the size changes slightly, since the equilibrium densities for different compositions differ slightly. However, these changes are insignificant, the resulting equilibrium concentrations (in mol L^{-1}) differ from the specified ones by less than 10%.

Fig. 1 shows the distribution of the solvent molecules around the protein as a function of the distance to its surface, the distance distribution functions (DDF). The distance to the surface of the protein is defined as the distance from the center of the solvent molecule (its center of mass) to the surface of the nearest heavy atom of the protein molecule (hydrogen atoms of the protein are not taken into account). The protein atoms were considered as spheres with radii equal to half of their Lennard-Jones parameter, σ, used in the molecular dynamics simulation, as in ref. 1.

Please note that the description of the distribution of solvent molecules relative to the surface of a large molecule (protein) by

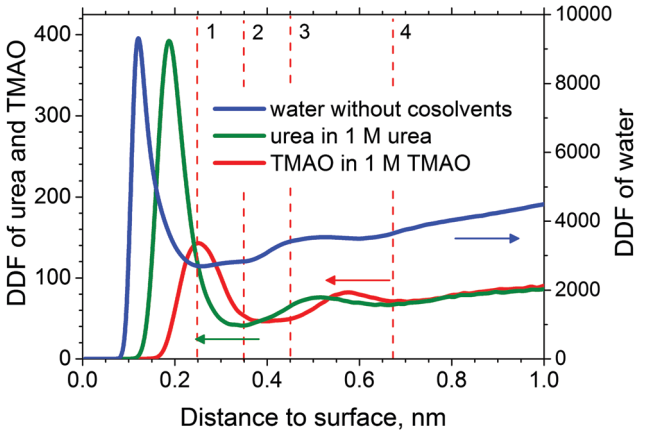

Fig. 1 Distribution functions of solvent molecules relative to the SNase surface (DDF): water in a solution without cosolvents (blue); urea at the concentration of 1 M (green); TMAO at 1 M (red). For water, the scale is shown on the right axis. Vertical dashed lines mark (here for TMAO) the position of the maximum of the first peak (numeral 1), the end of the first peak (2), the beginning of the second peak (3), and the end of the second peak (4).

the DDF, as shown above, differs from the widely used radial distribution function (RDF). The DDF provides directly the number of molecules within shells of unit thickness and approaches asymptotically a parabolic behavior, although only at distances that are larger than the size of the molecule (see ref. 1 for more details). The RDF is usually calculated for distances between centers and normalized to unity for large distances. Integrals over any distance interval gives the number of molecules in this interval. The coincidence of the asymptotes for urea and TMAO in Fig. 1 reflects the fact that the molar concentrations of these solutes are equal. Vertical dashed lines in Fig. 1 mark the boundaries of characteristic regions in the distribution of TMAO molecules near the protein. The vertical line which is marked with the numeral 1 shows the position of the maximum of the first DDF peak; it highlights the position of closest molecules (left slope). Line 2 marks the completion of the first peak, line 3 the beginning of the second peak, and line 4 indicates its completion. The values of these boundaries for TMAO as well as for urea and water are summarized in Table 1. The values given for the boundaries are auxiliary. Small variations do not affect the physical conclusions drawn, however. Recall that for water and the cosolvent we measure the distance to the surface of the nearest heavy protein atom, whereas in the literature this is also done to the center of the nearest atom[46,47] or to some selected atom or part of the protein.[35,48] Please note also

Table 1 Boundaries (in nm) of characteristic regions of the DDF function for different solvent molecules around SNase

	1	2	3	4
Molecule	Maximum of the first peak	End of the first peak	Beginning of the second peak	End of the second peak
Water	0.12	0.225	0.375	0.6
Urea	0.19	0.28	0.4	0.65
TMAO	0.25	0.35	0.45	0.68

that the cutoff for the hydration shell can be chosen differently, see as an example ref. 49 and references therein.

3. Methods and preliminary results

Local mobility of molecules near the protein

Following our recent work[22] to estimate the local translational mobility of molecules, we calculate their displacements over a certain, relatively small time interval, Δt:

$$\Delta \boldsymbol{r} = |\boldsymbol{r}(t_0 + \Delta t) - \boldsymbol{r}(t_0)|. \quad (1)$$

Recall that the distribution function of such displacements, averaged over all molecules of the liquid, presents the so-called "self-part" of the van Hove function.[39,40] This function is a tool, describing the dynamics of molecules in glasses and supercooled liquids, in particular, for studying glass transition processes,[50–52] including water.[53–55] However, here we are interested in the mobility of different molecules of a complex solvent mixture near the protein. Therefore, we consider it for different components of the solution (water, urea or TMAO) separately, using the same time interval Δt. In addition, we consider the molecules that are located at the moment t_0 in a narrow layer at a given distance R around the protein. Thereby, we extract the coordinates $\boldsymbol{r}(t_0)$ of the molecules whose centers are located at a moment t_0 in the interval $(R - \delta/2, R + \delta/2)$ around the protein. Then, for these molecules, we take from the molecular dynamics trajectories their coordinates $\boldsymbol{r}(t_0 + \Delta t)$ at time $t_0 + \Delta t$. The displacement Δr for each selected molecule is calculated by eqn (1). To improve the statistics, different time points along the molecular dynamics trajectories were used as t_0. Since our molecular dynamics trajectories are long enough and the used time intervals Δt are small (2 ps or 20 ps as in ref. 37), we obtain a reliable statistics for Δr even for cosolvents whose concentrations are relatively small. Fig. 2, adopted from ref. 37, shows the distribution of the displacements Δr over Δt = 2 ps for water molecules located initially in layers of width δ = 0.025 nm at different distances R.

The blue line corresponds to a distant layer, outside the hydration shell, *i.e.* in the bulk. The red line shows the distribution for a layer at the maximum of the second DDF peak of water, at $R \approx 0.48$ nm. One can see that the displacements of the water molecules at this distance differs little from the displacements in the bulk. However, at smaller distances, differences become noticeable, especially for the closest molecules (from the left slope of the first peak of the DDF, dashed curve). This calculation shows directly that the dynamics of water molecules near the protein is decreased, and the molecules move as in the bulk just beyond the second maximum of the DDF.

Please note that during the time interval Δt = 2 ps, most of the molecules leave their initial layer. This is seen in Fig. 2, where the layers are 0.025 nm thick and the spread of displacements is 0.4 nm or more. In ref. 37, it was shown that the use of the longer interval Δt = 20 ps leads to the same conclusions regarding the change in the mobility of molecules with distance from the protein as the use of Δt = 2 ps.

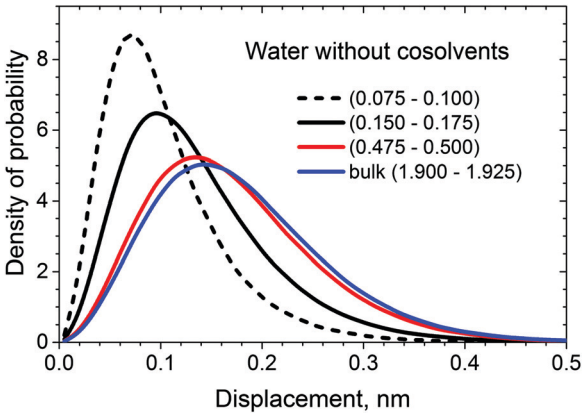

Fig. 2 Distribution of displacements of the water molecules over the time interval Δt = 2 ps. The molecules are initially located in narrow layers around the protein: 0.075–0.10 nm (dashed line), 0.15–0.175 (black), 0.475–0.50 (red) and 1.90–1.925 (blue).

To describe the altered mobility in the vicinity of the protein in more detail, we proposed to use the mean displacement of the molecules, $\langle \Delta r(R) \rangle$, in a constant time interval Δt instead of the van Hove distribution function.[37] It characterises the mean mobility of the molecules, $\langle \Delta r(R) \rangle / \Delta t$, as a function of the initial distance R, since the same time interval Δt is used for all distances. Thus, we obtain an additional quantitative parameter to characterize the dynamics of different solvent molecules as a function of the distance to the protein.

The distance dependence of such mean displacements for water, urea and TMAO in a ternary solvent (1 M TMAO + 2 M urea) are shown exemplarily in Fig. 3. The curve for water is fully consistent with previous conclusions about the dynamics of water molecules in the hydration shell of proteins.[16] Here, the same behavior is also observed for the cosolvents. Both urea and TMAO are markedly slowed down near the protein, and outside the second peak, their mobility reaches the bulk value.

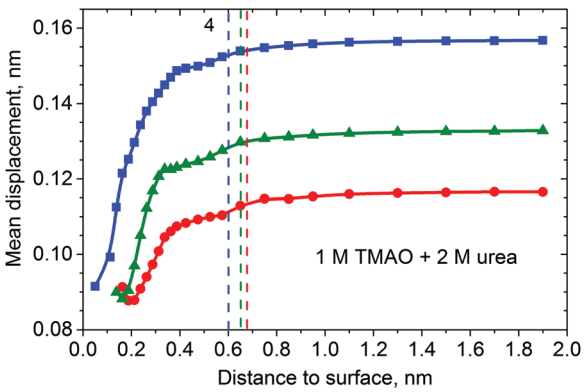

Fig. 3 Profiles of the mean displacements of solvent molecules around the protein SNase for Δt = 2 ps: water (blue), urea (green) and TMAO (red). Solvent: 1 M TMAO + 2 M urea. Vertical dashed lines show the completion of the second peaks in the DDF (see Table 1). The standard error bars for the data shown are less than the size of the symbols.

Additionally, we note that the change in the mobility of the molecules near a protein is non-linear. As shown in ref. 37, the derivatives of the profiles of the mean displacements reveal extrema, the positions of which correlate with the positions of the maxima in the DDF of the respective molecules.

Residence time in the hydration shell

To study the residence time (''lifetime'') of solvent molecules near the protein, we monitor the decrease of the number of the molecules initially located within a distance R of the protein, *i.e.*, a solvation shell of thickness R. When molecules cross the border of the hydration shell, they are considered as having left the shell, returning molecules are not taken into account. Also, new molecules entering the shell are not considered. Fig. 4 shows how the fraction of the initial water molecules, $N(t)/N(t_0)$, in the shells of different thicknesses change with time (decay curves). In ref. 56, we calculated similar curves for the neighboring atoms in Lennard-Jones liquids, leaving the nearest environment of an atom. These curves were well described by one exponent. Now, the situation is more complicated; the dotted line shows attempts to describe our decay curves by one exponential function. The solvent molecules around the protein are in different environments. Near the protein, they move slower due to steric effects, some molecules can be retained by hydrogen bonds with the protein, or are located in protein pockets. The existence of such ''stuck'' molecules is indicated by the very slow decay of the curves at large times in Fig. 4. Even in the case of a relatively thin layer, R = 0.25 nm (the region of the first DDF peak for water), a considerable fraction of the initial molecules remains even 1000 ps after the start of the observation.

The decay curves for water molecules, urea, and TMAO from the regions of their first DDF peak are shown on the same scale in Fig. 5 (the curve for water corresponds to the lower curve in Fig. 4). The inset shows the area near 1000 ps on an enlarged scale. We see that approximately 20 water and around 7 urea molecules still remain up to this time. This amount of stuck molecules is difficult to explain by simple diffusive types of motion.

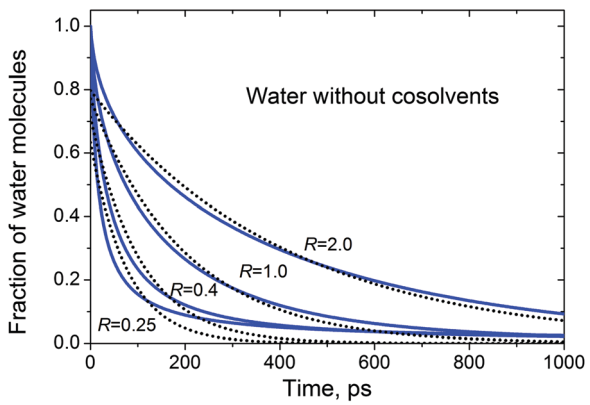

Fig. 4 Kinetics of the release of water molecules from hydration shells of different thickness around the protein. The boundary of a shell is defined as the surface located at a distance R from the surface of the protein. From bottom to top: R = 0.25, 0.4, 1.0 and 2 nm. Solid lines: molecular dynamics results, dotted lines: fit to an exponential function.

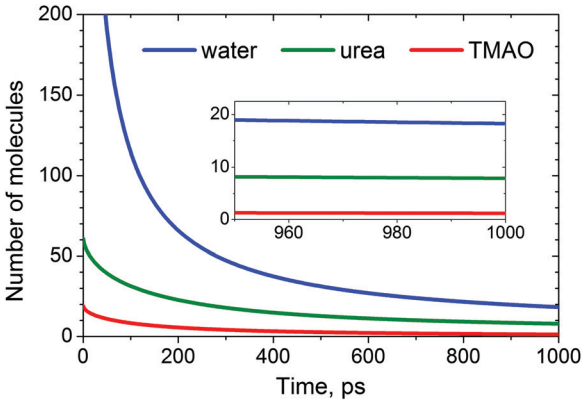

Fig. 5 Kinetics of the release of solvent molecules from solvation shells around SNase, which comprise the first maximum of the DDFs. From top to bottom: water, urea, TMAO. The inset shows the region near 1000 ps on an enlarged scale.

The observed decay curves for all components and different solvent compositions can be well fitted by the sum of three exponential functions and a time-independent term, n_∞:

$$N(t) = n_\infty + A_1\cdot\exp(-t/\tau_1) + A_2\cdot\exp(-t/\tau_2) + A_3\cdot\exp(-t/\tau_3). \quad (2)$$

The value obtained for n_∞ can be interpreted as the number of molecules still bound to the protein. For shells corresponding to the region of the first DDF peaks, these values are close to the residual values shown in the inset of Fig. 5. For thinner shells, the obtained value of n_∞ is smaller since there are initially fewer molecules in such shells. For thicker shells, the value of n_∞ increases slightly, but its determination by eqn (2) becomes less accurate.

Since it is not possible to describe our dynamic behavior by one exponential function and since we obtain from our fitting procedure three independent ''decay times'', the interpretation of which is not obvious, we use as characteristic time to describe the observed decay a half-time value, $\tau_{1/2}$, which is the time after which half of the initial molecules have left the shell, *i.e.* $N(\tau_{1/2}) = N(t_0)/2$. However, as some molecules are delayed for a long time, stuck close to the protein, it seems reasonable not to take such molecules into account when estimating the outflow of molecules from the shells. Hence, instead of the total number of initial particles, $N(t_0)$, we should use $N(t_0) - n_\infty$. Thereby, we obtain another half-time, $\tau_{1/2}^*$, determined from the condition $N(\tau_{1/2}^*) = (N(t_0) - n_\infty)/2$, the interpretation of which is not obvious, however, and different approaches might be possible to use.[57] Here, we use the half-time value $\tau_{1/2}^*$ to characterize the release kinetics. On the other hand, the differences between $\tau_{1/2}^*$ and $\tau_{1/2}$ are not really significant and do not lead to a qualitative change in our results. As in our studies of the displacements above, we plot the half-times $\tau_{1/2}^*$ and $\tau_{1/2}$ as a function of the shell thickness R. Fig. 6 compares the profiles $\tau_{1/2}^*(R)$ and $\tau_{1/2}(R)$ for water, urea and TMAO. The difference is noticeable only for urea (green lines),

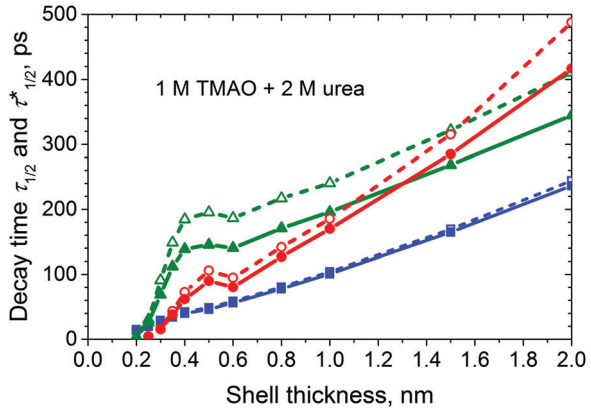

Fig. 6 Half-time profiles for $\tau_{1/2}$* (solid lines and full symbols) and for $\tau_{1/2}$ (dashed lines and empty symbols) for water (blue), urea (green) and TMAO (red) for the model used in Fig. 3.

since in this case the stuck molecules constitute a noticeable amount compared to $N(t_0)$ (about 20% at a concentration of 1 M for the layer corresponding to the first DDF peak). For water, the amount of such stuck molecules is only a few percent of the total number of water molecules in the shell, which is around 700. Therefore, the blue curves in Fig. 6 are almost identical. For TMAO, this correction is also not important since the number of stuck molecules is very small. Obviously, the half-time should increase with the thickness of the shell, since the molecules have to diffuse to an increasing distance. It is also clear that the molecules which are more mobile will leave the shell faster, *i.e.*, at the same thickness R, the half-time for the more mobile component will be less than that for the slower one. Fig. 6 confirms this for thick shells, *i.e.* for R larger than the hydration shell. We observe an universal increase in the curves for all models with R, and a correlation with the mobility: water molecules exit faster, followed by urea and then TMAO, according to their mobility (see Fig. 3). However, in the region of the hydration shell, the situation is more intricate, as discussed below.

Recall, see Section 2, for the averaging, we use each 2 ps the configuration of our models as the initial one (for the initial time t_0) and make averaging over all these decay curves. For the used MD trajectories of 40 ns, we have about 20 000 curves. Since the initial configurations are distributed uniformly along the trajectory, possible correlations between adjacent initial configurations should not affect the result. To verify this, we performed test calculations using configurations spaced by 1 ns as initial ones. In this case, we have only 40 decay curves that can be safely considered independent. It turned out that the

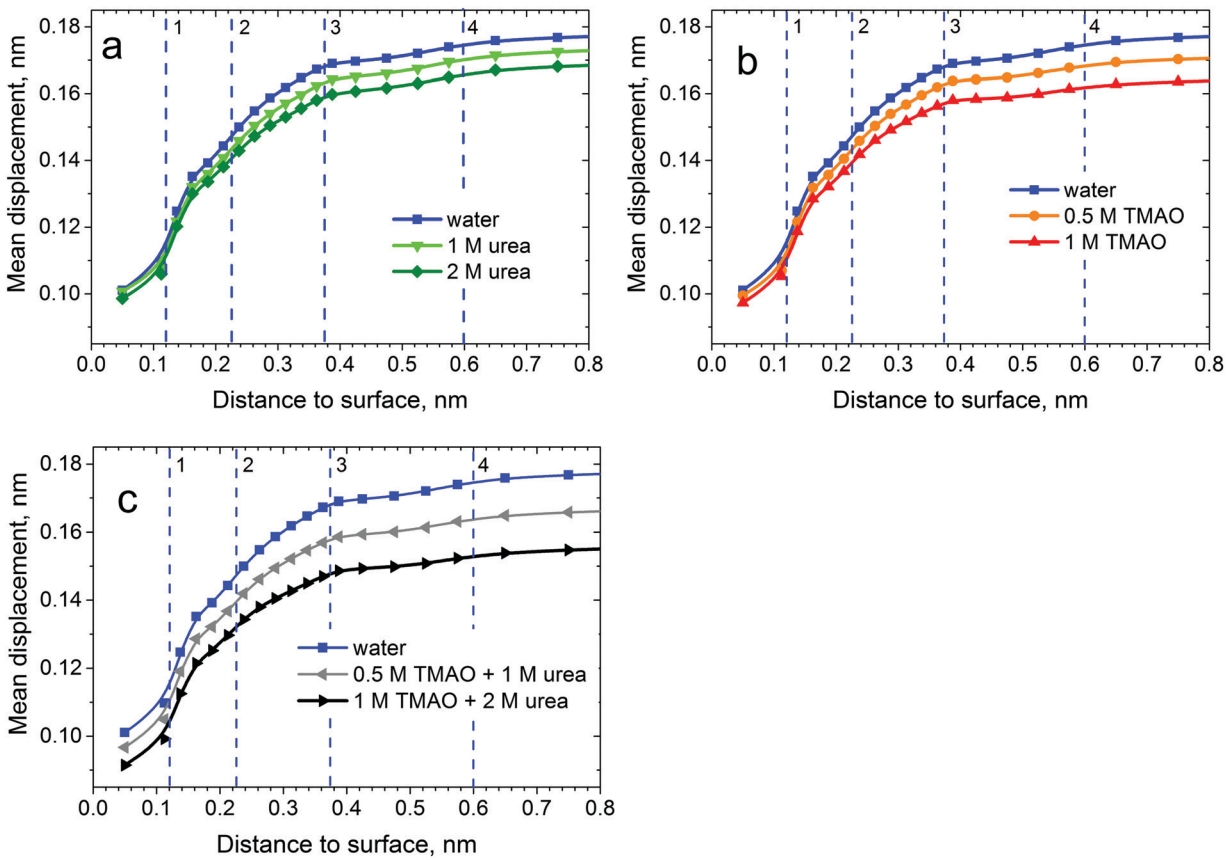

Fig. 7 Profiles of the mean displacements of water molecules within Δt = 2 ps in different solvents: (a) with urea (1 M and 2 M), (b) with TMAO (0.5 M and 1 M), (c) ternary solvents (0.5 M TMAO + 1 M urea and 1 M TMAO + 2 M urea). The upper blue curve in all the figures corresponds to water without cosolvents. Vertical dashed lines highlight the maxima of DDF for water (see Table 1). The standard error bars for the data shown are less than the size of the symbols.

mean decay curves both for water and cosolvents practically coincide with those shown in Fig. 4 and 5. The difference is only in the magnitude of the error bar. In the latter case, the error bar is of the order of the line thickness, and in the former case, it is much smaller. Thus, we obtain very smooth decay curves, which allows us to calculate the half-time value reliably. Our estimation shows that the error bar for the half-time profiles does not exceed the size of the symbol in the curves in Fig. 6. The accuracy of the n_∞ value is less since it is determined from fitting our decay curves using eqn (2).

4. Results and discussion – different solvent compositions

Translational motion

The profiles of the mean displacements of water molecules in solvents of different composition are compared in Fig. 7. The uppermost curve in the figures refers to the model where the solvent is water without cosolvents. The addition of urea (Fig. 7a) or TMAO (Fig. 7b) reduces the mobility of water both near the protein and further away. In the ternary solvents (Fig. 7c), the mobility of water additionally decreases in comparison to the binary solvents.

The addition of the cosolvents decreases the mobility of the water molecules in full correspondence with the changes of the self-diffusion coefficient of water in these solutions. Both, increasing the concentration and addition of the second cosolvent leads to a slowing down of the water molecules (see also the second column in the Table 2 taken from ref. 37). The self-diffusion coefficients, D, given in Table 2, should be compared with the behavior of the mean displacements for layers that are far away from the protein. Interestingly, Fig. 7 shows the same trend also near the protein: a decrease in the water mobility upon addition of the cosolvents. Also, the profiles in Fig. 7 for different solvent compositions do not intersect each other at all distances.

A closer inspection of Fig. 7 reveals a remarkable additivity of the influence of the cosolvents on the mobility of the water molecules. In particular, the decrease of the mean displacement of water in the solvent upon addition of 2 M urea (compared to water without cosolvents) is double the change for the 1 M urea solution. Similarly, the decrease in the mean displacement in the ternary solvent (for example, in 0.5 M TMAO + 1 M urea) is the sum of the changes for the binary solvent 0.5 M TMAO and 1 M urea. This indicates that, for the concentrations used, the cosolvent molecules act on the water dynamics independently.

The profiles of the mean displacements of urea and TMAO molecules within Δt = 2 ps are shown in Fig. 8a and b. In general, these curves are very similar to the ones for water. Outside the second peaks of the DDF (to the right of the 4th dashed lines), the displacement profiles for urea and TMAO for all solvent compositions reach asymptotic values which agree with the self-diffusion coefficients of these molecules in the bulk. In the region of the hydration shell, when approaching the protein, a universal decrease in mobility is observed, as for water (Fig. 7). The greatest change in mobility (a steep decline in the displacement profiles) is observed in the region of the first DDF peak (to the left of the 2nd dashed line), for both cosolvents and for water.

Table 2 Self-diffusion coefficients, D, for the water molecules and the cosolvents in an aqueous solution of SNase, calculated by the Einstein formula for times exceeding 1 ns (taken from ref. 37)

Composition of the solvent	D(water), nm^2 ps^{-1}	D(urea), nm^2 ps^{-1}	D(TMAO), nm^2 ps^{-1}
Pure water	0.00264	—	—
1 M urea	0.00246	0.00154	—
2 M urea	0.00226	0.00139	—
1 M TMAO	0.00206	—	0.00088
1 M TMAO + 2 M urea	0.00173	0.00109	0.00077

Solvent molecule outflow

For all our models, we calculated the delay curves $N(t)$ of the solvent molecules from shells around the protein. Table 3 depicts the values of the half-time, $\tau_{1/2}$*, and the numbers of stuck molecules, n_∞, for shells corresponding to the first DDF peaks of water, urea, and TMAO for different solvent

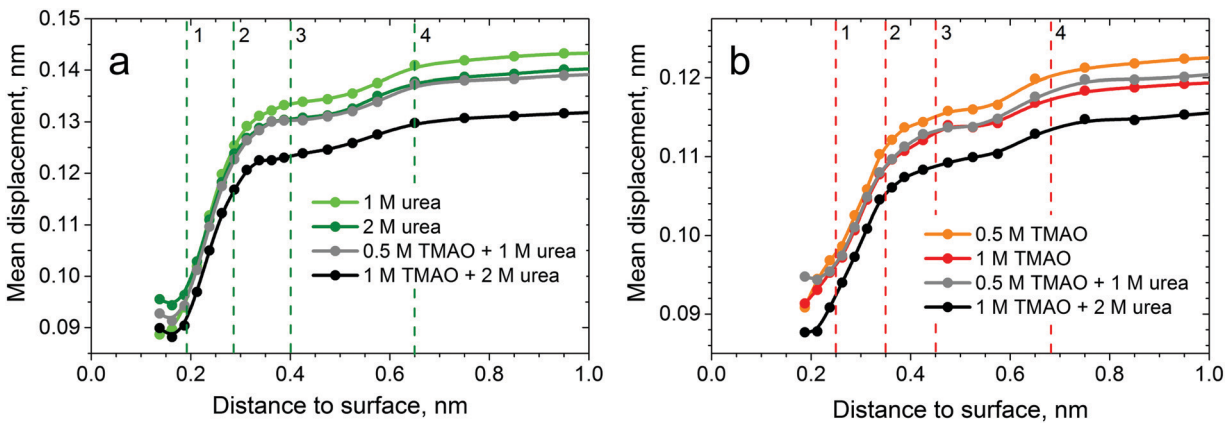

Fig. 8 Profiles of the mean displacements of urea (a) and TMAO (b) molecules in different solvents as a function of distance from the protein SNase. For urea: binary 1 M and 2 M (light and dark green curves), ternary: 0.5 M TMAO + 1 M urea and 1 M TMAO + 2 M urea (grey and black). For TMAO: binary 0.5 M and 1 M (orange and red curves), and the same ternary solvents.

Table 3 The half-time $\tau_{1/2}$* (in ps) of solvent molecules for the shell of the first DDF peak and the average number of molecules, n_∞, stuck at the protein, for water, urea and TMAO at different solvent compositions. The values in brackets show n_∞ as a fraction of the total number, $N(t_0)$, of solvent molecules in the shell (for water, urea and TMAO), see Section 3

Composition of the solvent	Parameter	Water	Urea	TMAO
Water without cosolvents	$\tau_{1/2}$*	14.8	—	—
	n_∞	18.34 (0.025)	—	—
1 M urea	$\tau_{1/2}$*	15.8	89.9	
	n_∞	14.01 (0.020)	6.44 (0.192)	
2 M urea	$\tau_{1/2}$*	15.9	83.3	—
	n_∞	17.21 (0.026)	6.43 (0.106)	—
0.5 M TMAO	$\tau_{1/2}$*	16.09	—	67.2
	n_∞	17.82 (0.025)	—	0.26 (0.031)
1 M TMAO	$\tau_{1/2}$*	16.87	—	67.5
	n_∞	17.85 (0.025)	—	0.80 (0.042)
0.5 M TMAO +	$\tau_{1/2}$*	16.7	92.24	60.2
1 M urea	n_∞	17.51 (0.027)	4.79 (0.149)	0.41 (0.051)
1 M TMAO +	$\tau_{1/2}$*	19.4	98.5	57.2
2 M urea	n_∞	26.67 (0.044)	8.88 (0.149)	1.57 (0.089)

compositions. Please recall that the values of n_∞ of the solutes are found by fitting the decay curves by eqn (2). After averaging over all solvent compositions, the mean values of n_∞ are equal to 18.50 ± 1.17 for water, 6.64 ± 0.75 for urea and 0. 76 ± 0.45 for TMAO. The model with a ternary solvent (1 M TMAO + 2 M urea) shows the largest deviation from the mean values. Excluding this model, we yield the values: 17.12 ± 0.52 for water, 5.89 ± 0.55 for urea, and 0.49 ± 0.16 for TMAO. In any case, with sufficient certainty we can say that nearly 20 water molecules and 6–7 urea molecules are delayed. On the other hand, we can assume that the TMAO molecules do not stay long near the protein, since the value of n_∞ is less than one. The principal difference between TMAO and urea is also seen from the fact that at the same molar concentration (1 M) in the binary solutions, the values of n_∞ are equal to 0.80 and 6.44, respectively (see Table 3).

We calculated also the half-times for layers of different thickness R. Fig. 9 shows the profiles obtained for water, urea and TMAO for different solvent compositions. For large R, the half-times unambiguously correlate with the mean displacement of molecules in the bulk: the greater the mobility of the molecules, the smaller is $\tau_{1/2}$*(R), *i.e.* such molecules leave layers of the same thickness faster (compare Fig. 7 and 9). This holds true for water and the cosolvents, and for all solvent compositions.

The profiles of the half-time $\tau_{1/2}$* for water behave monotonously up to the thinnest shells and do not intersect each other throughout the interval R considered (Fig. 9a). Please recall, the profiles of the mean displacements for water behave in a similar way for all models (Fig. 7). This means that the character of the dynamics of the water molecules in solutions of

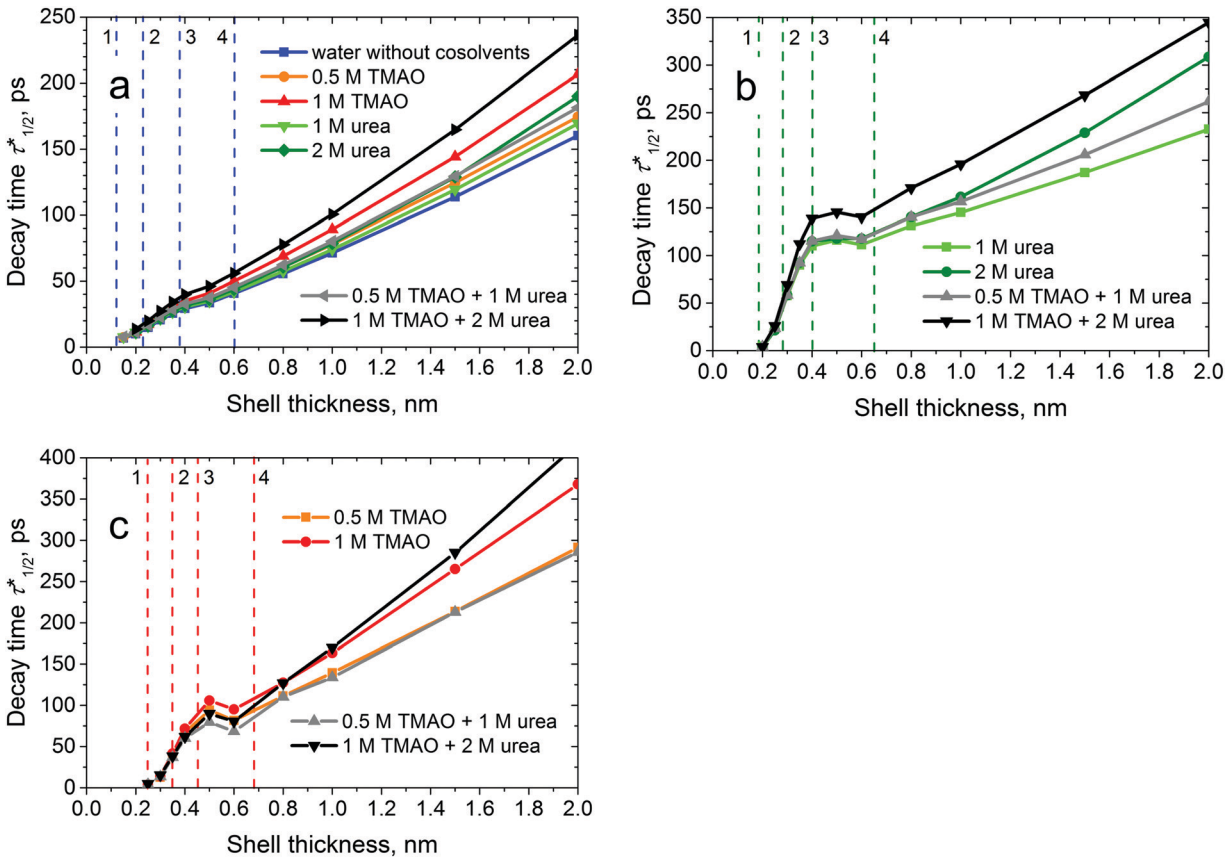

Fig. 9 Profiles of the half-time $\tau_{1/2}$* as a function of shell thickness around SNase for solvent molecules in solutions of different composition: water (a), urea (b), TMAO (c).

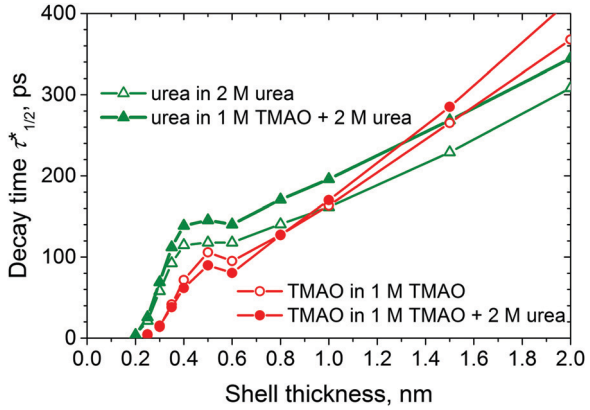

Fig. 10 Profiles of the half-time, $\tau_{1/2}$*, for urea (green triangles) and TMAO (red circles) near the surface of SNase for solutions of different composition.

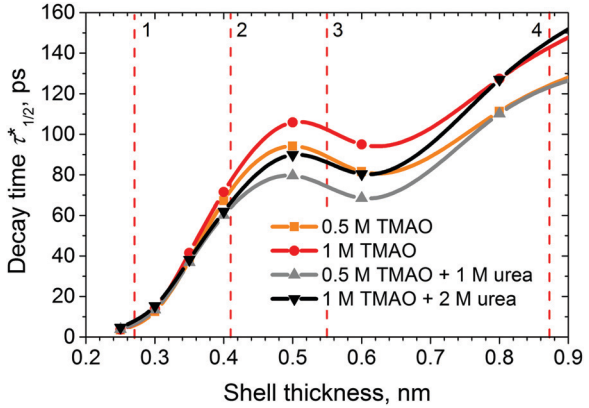

Fig. 11 Profiles of the half-time $\tau_{1/2}$* of TMAO for solutions of different composition: binary solvent: red and orange, ternary: black and grey (part of Fig. 9c on an enlarged scale).

different composition does not change markedly upon approaching the protein. However, the cosolvents behave differently near the protein. For urea (Fig. 9b), the curves exhibit a plateau in the region of the second peak of the DDF, and for TMAO, we observe a small maximum (Fig. 9c). Interestingly, these features of the cosolvent profiles exist for all solvent compositions.

Fig. 10 presents the profiles $\tau_{1/2}$*(R) for urea and TMAO both for the ternary and binary solvents. The pairs of curves characterize the range of differences of the data for all our solvent compositions. In particular, we notice the principal difference between the behavior of TMAO and urea and the seemingly contradictory fact that the slower TMAO molecules (in terms of displacements, as shown in Fig. 3 and 8) have smaller values of $\tau_{1/2}$* near the protein, *i.e.* they leave the protein faster than the urea molecules, which are more mobile in this area. But this result would be in complete agreement with the fact that the concentration of TMAO is reduced in the vicinity of the protein compared to urea. However, the reason for such a dynamic behavior of the cosolvents near the protein remains unclear. We could, for instance, expect that near the protein the displacement of molecules is anisotropic. For example, the urea molecules might prefer to move along the protein surface and the TMAO molecules, on the contrary, move mainly in the "radial" direction. However, our analysis does not confirm this idea. We calculated the normal and tangential components of the displacements of the urea and TMAO molecules near the protein and did not find any clear excess in one or the other direction. Hence, the observed contradiction between the translational mobility and the lifetime of the cosolvents near the protein requires additional investigations.

Our dynamics analysis discloses also another interesting fact regarding the mutual influence of urea and TMAO in the hydration shell of the protein. The addition of urea contributes to a decrease of TMAO near the protein compared to the bulk behavior (see also ref. 1). Fig. 11 shows the profiles of the half-time $\tau_{1/2}$* for TMAO on an enlarged scale. In the region of the maximum, the longest half-time is observed for the binary solvents, for the ternary ones, the half-time is shorter. This can be understood if one assumes that the addition of urea accelerates the release of TMAO molecules from the environment of the protein, *i.e.* reduces its residence time near the protein. In ref. 1, this conclusion was based on a comparison of the volume fraction occupied by TMAO molecules near the protein in binary and ternary solutions. Here, we can confirm this fact, considering the dynamics of the molecules at play.

5. Conclusions

We studied the dynamic behavior of molecules in the hydration shell of the globular protein SNase in aqueous solutions with different contents of cosolvents (urea and TMAO) by calculating the mean displacement of molecules at different distances from the protein and the characteristic lifetimes of the molecules in solvation shells of different thicknesses. To characterize the observed displacements in more detail, the self-part of the van Hove function was determined, which is generally used in studies of the dynamics in bulk liquids and glasses. Here, we calculated the individual displacements $\Delta r(R)$ within a fixed small time interval (Δt = 2 ps) for molecules originally located in a given narrow layer at a given distance R from the protein interface. The distribution of such displacements allows us to compare the mobility of different components of the solvent depending on the distance to the protein. To estimate the characteristic lifetime of molecules near the protein, we monitored the change in the number of molecules that were originally inside a solvation shell with a given thickness R. As a quantitative estimate of the rate of release, we used the period of time where half of the initial molecules has left, the so-called half-time, $\tau_{1/2}$*.

The parameters considered reflect different aspects of the dynamic behavior of the molecules in the hydration shell of the protein. Their combined consideration allows us to reveal additional features of the dynamic behavior of the cosolvents. The results obtained are fully consistent with prevalent ideas about the dynamics of water molecules around biomacromolecules such as proteins, as studied in many papers (for example, see the review ref. 16): the mobility of water molecules decreases

several times as they approach the protein when compared to the mobility in the bulk, and this occurs in the immediate vicinity of the protein, *i.e.* within the first two layers of water molecules. We show that the two selected cosolvents, urea and TMAO, experience a similar retardation at the same distances, *i.e.* up to 0.8–1.0 nm from the protein surface. This coincidence suggests that the mobility of the cosolvent molecules is primarily determined by the mobility of the water in which they are embedded.

The half-times $\tau_{1/2}$* for large R are clearly correlated with the mean displacement of the molecules, $\langle \Delta r(R) \rangle$. Molecules leave a layer the faster, the higher their mobility. This holds true both for water and the cosolvents as well as for all solvent compositions. For water, this correspondence is valid over the whole distance (R) range investigated. This means that the dynamic properties of water do not change qualitatively when approaching the protein, regardless of the cosolvents added. There is only a gradual slowing down, depending on the self-diffusion coefficient of water in the solution of a given composition.

For the cosolvents, a similar monotonic behavior of the mean displacement $\langle \Delta r(R) \rangle$ is observed for large R. However, the $\tau_{1/2}$* values behave differently near the protein. For urea, we observe a plateau, and for TMAO a shallow maximum in the distance profiles of $\tau_{1/2}$* in the region of the second peak of their distribution functions around the protein. Interestingly, the half-time for TMAO is shorter than for urea in this region. This means that the TMAO molecules exit faster from the protein's hydration shell than urea, despite the fact that the mobility (defined as the mean displacement of molecules for the same period of time) of TMAO is lower than that of urea in this area. This behavior is observed for all solvent compositions studied and reflects the observation that the fraction of urea near the protein is higher than for TMAO.

An additional interesting finding is that the half-time for TMAO is shorter in the ternary solvents (TMAO + urea + H_2O) than in the binary ones (TMAO or urea + H_2O) near the protein. This indicates that in the presence of urea, which tends to interact preferentially with the protein interface, TMAO escapes from the protein faster. This is consistent with a recent finding that the fraction of TMAO near the protein decreases in the presence of urea.[1] The reason for such a behavior of the cosolvent molecules in the vicinity of the protein is not fully understood, however. As it was shown recently in ref. 14, in ternary aqueous solutions (in the absence of a protein), TMAO and urea do not affect the mutual distribution of the other cosolvent. This indicates that the behavior of the cosolvents in the hydration shell is caused primarily by the protein, and not by the interaction of urea and TMAO with each other.

From the analysis of the decrease of the number of particles initially located in the hydration shell, we can conclude that some molecules remain near the protein for a rather long time. We estimated that for shells with a thickness corresponding to the width of the first peak of the distribution function, about 20 water molecules and 6–7 urea molecules are delayed more than 1000 ps for all solvent compositions studied. This can be considered as a result of the direct interaction of water and urea with the protein. The number of such molecules for TMAO is estimated to be less than one. This is in line with the well-known property of effective osmolyte-protectors such as TMAO to avoid direct interaction with the protein, also denoted as osmophobic effect.[4,7]

Conflicts of interest

There are no conflicts of interest to declare.

Acknowledgements

Financial support from grant RFBR (No. 18-03-00045) is gratefully acknowledged. R. W. acknowledges funding from the Cluster of Excellence RESOLV (Deutsche Forschungs-gemeinschaft (DFG, German Research Foundation) under Germany's Excellence Strategy, EXC-2033, Projektnummer 39067787).

References

1 N. Smolin, V. P. Voloshin, A. V. Anikeenko, A. Geiger, R. Winter and N. N. Medvedev, *Phys. Chem. Chem. Phys.*, 2017, **19**, 6345–6357.
2 P. H. Yancey, M. E. Clark, S. C. Hand, R. D. Bowlus and G. N. Somero, *Science*, 1982, **217**, 1214–1222.
3 D. R. Canchi, P. Jayasimha, D. C. Rau, G. I. Makhatadze and F. E. Garcia, *J. Phys. Chem. B*, 2012, **116**, 12095–12104.
4 M. Gao, C. Held, S. Patra, L. Arns, G. Sadowski and R. Winter, *ChemPhysChem*, 2017, **18**, 2951–2972.
5 E. Schneck, D. Horinek and R. R. Netz, *J. Phys. Chem. B*, 2013, **117**, 8310–8321.
6 B. Moeser and D. Horinek, *J. Phys. Chem. B*, 2014, **118**, 107–114.
7 D. R. Canchi and A. E. Garcia, *Annu. Rev. Phys. Chem.*, 2013, **64**, 273–293.
8 D. W. Bolen and G. Rose, *Annu. Rev. Biochem.*, 2008, **77**, 339–362.
9 L. Larini and J.-E. Shea, *J. Phys. Chem. B*, 2013, **117**, 13268–13277.
10 M. V. Fedotova, S. E. Kruchinin and G. N. Chuev, *New J. Chem.*, 2017, **41**, 1219–1228.
11 D. W. Bolen and I. V. Baskakov, *J. Mol. Biol.*, 2001, **310**, 955–963.
12 S. Paul and G. N. Patey, *J. Phys. Chem. B*, 2007, **111**, 7932–7933.
13 P. Ganguly, T. Hajari, J.-E. Shea and N. F. A. van der Vegt, *J. Phys. Chem. Lett.*, 2015, **6**, 581–585.
14 E. D. Kadtsyn, A. V. Anikeenko and N. N. Medvedev, *J. Struct. Chem.*, 2018, **59**, 347–354.
15 B. Bagchi, *Chem. Rev.*, 2005, **105**, 3197–3219.
16 D. Laage, T. Elsaesser and J. T. Hynes, *Chem. Rev.*, 2017, **117**, 10694–10725.
17 A. Geiger, A. Rahman and F. H. Stillinger, *J. Chem. Phys.*, 1979, **70**, 263–276.
18 A. Geiger, *Ber. Bunsenges. Phys. Chem.*, 1981, **85**, 52–63.
19 P. Ahlstoem, O. Teleman and B. Joenson, *J. Am. Chem. Soc.*, 1988, **110**, 4198–4203.

20 A. R. Bizzarri and S. Cannistraro, *Phys. Rev. E: Stat. Phys., Plasmas, Fluids, Relat. Interdiscip. Top.*, 1996, **53**, R3040–R3043.
21 V. A. Makarov, M. Feig, B. K. Andrews and B. M. Pettitt, *Biophys. J.*, 1998, **75**, 150–158.
22 S. G. Dastidar and C. Mukhopadhyay, *Phys. Rev. E: Stat., Nonlinear, Soft Matter Phys.*, 2003, **68**, 021921.
23 P. Rani and P. Biswas, *J. Phys. Chem. B*, 2015, **119**, 13262–13270.
24 J. N. Dahanayake, E. Shahryari, K. M. Roberts, M. E. Heikes, C. Kasireddy and K. R. Mitchell-Koch, *J. Chem. Inf. Model.*, 2019, **59**, 2407–2422.
25 R. S. Taylor, L. X. Dang and B. C. Garrett, *J. Phys. Chem.*, 1996, **100**, 11720–11725.
26 R. Abseher, H. Schreiber and O. Steinhauser, *Proteins: Struct., Funct., Genet.*, 1996, **25**, 366–378.
27 E. Chiavazzo, M. Fasano, P. Asinari and P. Decuzzi, *Nat. Commun.*, 2014, **5**, 3565.
28 P. Liu, E. Harder and B. Berne, *J. Phys. Chem. B*, 2004, **108**, 6595–6602.
29 A. J. Campbell, M. L. Lamb and D. J. McCarthy, *J. Chem. Inf. Model.*, 2014, **547**, 2127–2138.
30 S. Uehara and S. Tanaka, *J. Chem. Inf. Model.*, 2017, **574**, 742–756.
31 K. Julius, J. Weine, M. Berghaus, N. König, M. Gao, J. Latarius, M. Paulus, M. A. Schroer, M. Tolan and R. Winter, *Phys. Rev. Lett.*, 2018, **121**, 038101.
32 M. A. Schroer, Y. Zhai, D. C. F. Wieland, C. J. Sahle, J. Nase, M. Paulus, M. Tolan and R. Winter, *Angew. Chem., Int. Ed.*, 2011, **50**, 11413–11416.
33 D. Huang, E. Rossini, S. Steiner and A. Caflisch, *ChemMedChem*, 2014, **9**, 573–579.
34 S. Moelbert, B. Normand and P. De Los Rios, *Biophys. Chem.*, 2005, **112**, 45–57.
35 N. F. A. van der Vegt and D. Nayar, *J. Phys. Chem. B*, 2017, **121**, 9986–9998.
36 J. T. King, E. J. Arthur, C. L. Brooks and K. J. Kubarych, *J. Phys. Chem. B*, 2012, **116**, 5604–5611.
37 V. P. Voloshin and N. N. Medvedev, *J. Struct. Chem.*, 2019, **60**, 942–951.
38 N. Smolin and R. Winter, *J. Phys. Chem. B*, 2008, **112**, 997–1006.
39 L. van Hove, *Phys. Rev.*, 1954, **95**, 249–262.
40 P. Hopkins, A. Fortini, A. J. Archer and M. Schmidt, *J. Chem. Phys.*, 2010, **133**, 224505.
41 B. Hess, C. Kutzner, D. van der Spoel and E. Lindahl, *J. Chem. Theory Comput.*, 2008, **4**, 435–447.
42 S. Pronk, S. Pall, R. Schulz, P. Larsson, P. Bjelkmar, R. Apostolov, M. R. Shirts, J. C. Smith, P. M. Kasson, D. van der Spoel, B. Hess and E. Lindahl, *Bioinformatics*, 2013, **29**, 845–854.
43 W. L. Jorgensen, D. S. Maxwell and J. Tirado-Rives, *J. Am. Chem. Soc.*, 1996, **118**, 11225–11236.
44 H. J. C. Berendsen, J. R. Grigera and T. P. Straatsma, *J. Phys. Chem.*, 1987, **91**, 6269–6271.
45 S. Weerasinghe and P. E. Smith, *J. Phys. Chem. B*, 2003, **107**, 3891–3898.
46 X. Chen, I. Weber and R. W. Harrison, *J. Phys. Chem. B*, 2008, **112**, 12073–12080.
47 N. Bhattacharjee and P. Biswas, *Biophys. Chem.*, 2011, **158**, 73–80.
48 P. Rani and P. Biswas, *J. Phys.: Condens. Matter*, 2014, **26**, 335102.
49 F. Persson, P. Soederhjelm and B. Halle, *J. Chem. Phys.*, 2018, **148**, 215101.
50 W. Kob and H. C. Andersen, *Phys. Rev. E: Stat. Phys., Plasmas, Fluids, Relat. Interdiscip. Top.*, 1995, **51**, 4626–4641.
51 P. Gallo, R. Pellarin and M. Rovere, *Phys. Rev. E: Stat., Nonlinear, Soft Matter Phys.*, 2003, **67**, 041202.
52 B. P. Bhowmik, I. Tah and S. Karmakar, *Phys. Rev. E*, 2018, **98**, 022122.
53 F. Sciortino, P. Gallo, P. Tartaglia and S.-H. Chen, *Phys. Rev. E: Stat. Phys., Plasmas, Fluids, Relat. Interdiscip. Top.*, 1996, **54**, 6331–6343.
54 D. Paschek and A. Geiger, *J. Phys. Chem. B*, 1999, **103**, 4139–4146.
55 M. De Marzio, G. Camisasca, M. Rovere and P. Gallo, *J. Chem. Phys.*, 2017, **146**, 084502.
56 N. N. Medvedev, A. Appelhagen and A. Geiger, *Dokl. Akad. Nauk*, 1993, **332**, 191–194.
57 J. Schnitker and A. Geiger, *Z. Phys. Chem.*, 1987, **155**, 29–54.